Comparison of radiologic characteristics and pathological presentations of primary pulmonary lymphoma in 22 patients

**Yanchao Wang[1],*, Jun Han[2],* ⓘ,
Fantao Zhang[3],*, Zhaoyu Wang[4], Dahai Zhao[5],
Xuan Wang[6], Ningxin Wu[7], Rongjian Lu[8],
Chongchong Wu[9], Jie Gao[10], Lei Pan[11] and
Xinying Xue[11]**

Abstract

Objective: This study was performed to compare the radiologic characteristics and pathological presentations of primary pulmonary lymphoma (PPL), explore the possible mechanism underlying its development, summarize its radiologic characteristics, and improve the accuracy of its diagnosis.

Methods: The medical records of 22 patients pathologically diagnosed with PPL were retrospectively analyzed.

[1]Department of CT/MRI Center, People's Hospital of Wuwei city, Gansu, China
[2]Department of Radiology, The Third Affiliated Hospital of Chongqing Medical University, Chongqing, China
[3]Department of Radiology, Shengli Oilfield Central Hospital of Dongying city, Shandong, China
[4]Department of Pathology, Zhoushan Hospital, Zhejiang, China
[5]Department of Respiratory Medicine, The Second Hospital of Anhui Medical University, Anhui, China
[6]Department of Psychiatry, Beijing Huilongguan Hospital, Beijing, China
[7]Department of Cadres, 971 Hospital of the Chinese People's Liberation Army Navy, Beijing, China
[8]Department of Stomatology, Chinese PLA 307th Hospital, Beijing, China

[9]Department of Radiology, General Hospital of PLA, Beijing, China
[10]Department of Pathology, General Hospital of PLA, Beijing, China
[11]Department of Respiratory Medicine, Beijing Shijitan Hospital, Capital Medical University, Beijing, China

*These authors contributed equally to this work.

Corresponding author:
Xinying Xue, Department of Respiratory Medicine, Beijing Shijitan Hospital, Capital Medical University, No. 10 Tieyi Road, Yangfangdian, Haidian District, Beijing 100038, China.
Email: xinyingxue2010@163.com

Results: Chest computed tomography (CT) demonstrated single or multiple nodules and masses in the lungs, patchy opacities or consolidation along the bronchovascular bundle, and no significantly enlarged mediastinal or hilar lymph nodes. All 22 cases of PPL were classified as non-Hodgkin's lymphoma (NHL) by transbronchial biopsy, CT-guided needle biopsy, and postoperative pathology. Most (16 cases) were marginal-zone B-cell lymphomas of mucosa-associated lymphoid tissue (MALT). Twelve patients had air bronchograms within the lesion, and 13 showed ill-defined lesions with ground-glass brush-like changes.

Conclusion: PPL is a rare lung tumor, and most are classified as MALT lymphoma, a subtype of NHL. Chest CT can help to diagnose this disease. Positron emission tomography (PET)/CT is of great clinical value for evaluation of the lesion and patient's general condition. The possibility of PPL should be considered in patients with characteristic CT and PET/CT findings and mild clinical symptoms, and early treatment should be administered.

Introduction

Primary pulmonary lymphoma (PPL), a rare malignant tumor arising from lymph nodes or extranodal lymphoid tissues, represents 0.5% of all primary pulmonary neoplasms,[1,2] 0.4% of all lymphomas,[3] and 3.6% of all extranodal lymphomas.[4] There are two main groups of lymphomas: Hodgkin's lymphoma and non-Hodgkin's lymphoma (NHL). Subtypes of primary NHL include mucosa-associated lymphoid tissue (MALT) lymphoma, highly malignant large B-cell lymphoma, angiocentric lymphoma, and other rare subtypes such as intravascular lymphoma. Among them, MALT is the most common, accounting for 60% to 80% of all primary lung lymphomas; diffuse large B-cell lymphoma is the second most common, accounting for 10% to 25% of all primary lung lymphomas.[5] Most of the above-mentioned subtypes are low-grade malignant small B-cell MALT lymphomas. MALT lymphomas are now classified as extranodal marginal-zone B-cell lymphomas in the Revised European-American Lymphoma Classification. Most lung lesions that were previously termed "pseudolymphomas" are now also thought to represent pulmonary MALT lymphomas.[6] We used the diagnostic criteria developed by Cordier et al.[7] in 1993: (1) the lung and bronchus are involved without evidence of mediastinal adenopathy on the chest radiographs; (2) extrathoracic lymphoma was not previously diagnosed; (3) there is no evidence of extrapulmonary lymphoma or lymphocytic leukemia in the clinical examination, radionuclide bone scanning, computed tomography (CT) or lymphangiography, bone marrow examination, or positron emission tomography (PET)/CT; and (4) there is no evidence of extrathoracic disease up to 3 months after the initial diagnosis. Patients who fulfill all four criteria are diagnosed with PPL. A better understanding of PPL is urgently required. The present study was performed to explore the

possible mechanism underlying its development, summarize its radiologic characteristics, and improve the accuracy of its diagnosis.

Patients and methods

Patient studies

Data were collected from patients who showed pulmonary lesions in their CT images, which were obtained with a GE LightSpeed 64-Slice CT scanner (GE Healthcare, Chicago, IL, USA) from May 2009 to March 2017 in three grade-A tertiary hospitals in Beijing. All patients were pathologically diagnosed with PPL after CT-guided needle biopsy, surgical removal, or transbronchial biopsy. In the preoperative diagnosis and postoperative follow-up examination, all 22 patients underwent either a routine CT scan (5-mm thickness and 5-mm spacing between slices) or thin-slice chest CT scan (1.25-mm thickness and 1.25-mm spacing between slices). Multiplanar reformation, curved planar reformation, and volume rendering were performed after the detection of lesions, which were viewed in the mediastinal window and lung window. Prior to presentation, half of the patients underwent an ^{18}F-fluorodeoxyglucose (^{18}F-FDG) PET/CT scan using a Discovery ST PET/CT scanner (GE Healthcare). The PET data were acquired in three-dimensional mode for 2.5 minutes per bed in three or six bed positions, covering the entire chest. The acquired images were reconstructed by the Fourier rebinning ordered subsets expectation-maximization algorithm with attenuation correction. Before the examination, the doctor checked the patient's fasting blood glucose level. The patients were also asked to empty their urine and remove metal foreign bodies. The maximum standardized uptake value (SUVmax) was measured at the highest radioactivity concentration.

All patients' data were reviewed and their radiological manifestations and pathological characteristics were correlated to improve the understanding and diagnosis of PPL and reduce the misdiagnosis rate and time from misdiagnosis to correct diagnosis.

CT analysis

A thoracic radiologist with 15 years of experience in pulmonary imaging (C.W.) and a radiologist dedicated to chest imaging with 6 years of experience in pulmonary imaging diagnosis (J.H.) reviewed the CT images. If differences in opinion were encountered, the radiologists resolved them through consensus.

Statistical analysis

Data were analyzed using SPSS version 20.0 (IBM Statistics, Armonk, NY, USA). Age is expressed as mean ± standard deviation with range. The Kolmogorov–Smirnov test was used for data with a normal distribution.

Results

During the 8-year study period, 22 patients were included in this study (10 men and 12 women) (Table 1) with a mean age of 60 ± 5 years (range, 45–75 years). Eight patients had a history of smoking, and the remaining 14 patients were nonsmokers. Seven patients had no symptoms; one of these seven patients had a 20-year history of lupus nephritis, diabetes, and rheumatoid arthritis and had received regular treatment. Among the remaining 15 patients, 2 had a fever, 9 had productive phlegm, 4 had chest pain, 1 had blood-tinged sputum, and 2 had chest distress and shortness of breath. Physical examination revealed diminished breath sounds on the affected side in two patients; the other patients had no abnormalities. The 22 patients had been

Table I. Patients' clinical, radiologic, and pathological data

No./Age/Sex	Smoking history	Symptoms	Characteristics and distribution of lesions	Tumor size	Source of specimen	Pathological diagnosis	PET-SUV SUVmax	Treatment	Prognosis
1/63 years/Female	No	Productive phlegm	Nodules and masses in the RUL, RML, RLL, and LLL	7.6 × 8.6 cm	Bronchoscopy	MALT	3.86	R-COP chemotherapy	PET/CT following three cycles of chemotherapy demonstrated metabolic activity in the lesion. Subsequently, after three cycles of R-F chemotherapy, the patient had pulmonary infection and received anti-infection treatment.
2/57 years/Female	No	Fever and productive phlegm	Patches and masses in the RUL, RML, and RLL	12.3 × 8.5 cm	CT-guided needle biopsy	MALT	5.1	R-CHOP	After three cycles of chemotherapy, the productive phlegm disappeared. After another three cycles of chemotherapy, PET/CT demonstrated reduced consolidation in the right lung and a diminished metabolic rate.
3/53 years/Male	20–30 cigarettes/day for 30 years	No	Patches and plaques of ground-glass opacities in BL	6.2 × 2.9 cm	CT-guided needle biopsy	MALT	2.23–3.65	CHOP	CT following six cycles of chemotherapy demonstrated multiple bands in the lungs and a smaller lesion.
4/64 years/Male	20 cigarettes/day for 40 years	Productive phlegm and blood-tinged sputum with left chest pain	Honeycomb in the LLL	7.9 × 6.1 cm	Surgical removal	MALT		Surgical removal	Clinical follow-up
5/49 years/Male	No	Productive phlegm and frothy mucus	Patches of ground-glass opacities in the RUL and LUL	4.3 × 2.8 cm	Surgical removal of the lesion in the right upper lobe	MALT		Right upper lobe lobectomy	PET/CT scanning performed after three cycles of R-CHOP chemotherapy and four cycles of autologous CIK cell-based immunotherapy revealed multiple areas of consolidation in the lungs with irregular concentration of radioactivity, not excluding the possibility of residual malignancy.

(continued)

Table 1. Continued.

No./Age/Sex	Smoking history	Symptoms	Characteristics and distribution of lesions	Tumor size	Source of specimen	Pathological diagnosis	PET-SUV SUVmax	Treatment	Prognosis
6/45 years/Male	20 cigarettes/day for >20 years	Physical findings	Nodules in the RUL, RLL, and LLL	5.0 × 2.7 cm (maximum lesion)	CT-guided needle biopsy	MALT	7.7	R-CHOP chemotherapy	PET/CT following six cycles of chemotherapy showed significantly decreased bilateral parenchymal lung and pleural lesions and a diminished metabolic rate, and a CT scan performed in the local hospital 2 years later showed enlarged masses. The possibility of relapse could not be excluded.
7/63 years/Male	20 cigarettes/day for >40 years	Physical findings	Nodules in the RUL	2.3 × 2.1 cm	Surgical removal	MALT		Surgical removal	Clinical follow-up
8/59 years/Female	No	Cough	Nodules in the LLL	3.2 × 2.3 cm	CT-guided needle biopsy	MALT		R-COP chemotherapy	The patient demanded discharge after three cycles of chemotherapy.
9/61 years/Female	No	Physical examination	Masses in the LUL	5.7 × 3.5 cm	CT-guided needle biopsy	DLBCL	19.6	R-CHOP chemotherapy	After two cycles of chemotherapy, PET/CT demonstrated a reduced lesion size and diminished metabolic rate. After four cycles, PET/CT demonstrated a reduced lesion size and diminished metabolic rate. After five cycles, the patient developed fungal infection and was given antifungal treatment.
10/59 years/Female	No	Fever and chest distress	Patchy and nodular opacities in BL	5.2 × 4.4 cm	CT-guided needle biopsy	NK/T-cell lymphoma	11.8	Discharge when terminally ill	Treatment withdrawn

Table 1. Continued.

No./Age/Sex	Smoking history	Symptoms	Characteristics and distribution of lesions	Tumor size	Source of specimen	Pathological diagnosis	PET-SUV SUVmax	Treatment	Prognosis
11/61 years/Female	No	Cough	Nodular masses in the LUL, RLL, and LLL	2.2 × 2.2 cm (maximum lesion)	CT-guided needle biopsy	NK/T-cell lymphoma, nasal type	13	CHOP-L chemotherapy	After two cycles of chemotherapy, the fever and cough disappeared, fatigue improved, and PET/CT demonstrated a reduced lesion size and diminished metabolic rate
12/75 years/Female	No	Pain in the pharynx and dry cough	Large masses in the RUL, and RML	12.9 × 7.5 cm	CT-guided needle biopsy	T-cell lymphoma	5.73–9.34	COP+L chemotherapy	Patient died following exacerbation after chemotherapy
13/ 67 years/Male	>20 years	Productive phlegm, hemoptysis, and chest pain	Nodules in the LUL	2.0 × 3.4 cm	Surgical removal (left upper lobe)	DLBCL		Surgical removal	Clinical follow-up
14/58 years/Female	>30 years	Physical examination findings	Masses and nodules in the RUL	7.5 × 3.5 cm	CT-guided needle biopsy	DLBCL	19.5	Four cycles of CHOP chemotherapy, two cycles of MICE chemotherapy, and R-DHAP chemotherapy	PET/CT revealed reduced lesion volume in the right upper lobe, slightly diminished metabolic rate, and tumor viability
15/56 years/Male	>30 years	Intermittent cough	Multiple lung nodules and masses in the RLL, LUL, and LLL	6.2 × 5.0 cm	CT-guided needle biopsy	MALT		Treatment after discharge	Telephone follow-up
16/55 years/Male	No	Physical examination	Soft tissue masses in the RLL	5.6 × 4.3 cm	CT-guided needle biopsy	MALT		Four cycles of R-CHOP, two cycles of R-FCM, and maintenance treatment with rituximab	PET/CT following four cycles of R-CHOP chemotherapy suggested PR. PET/CT following two cycles of R-FCM chemotherapy revealed a CMR DS score of two points.
17/57 years/Female	No	Physical findings	Patchy ground-glass opacities in the RUL	5.6 × 2.3 cm	Surgical removal	MALT		Surgical removal	Telephone follow-up
18/54 years/Male	No	Chest pain for 3 years	LLL masses	5.7 × 3.2 cm	Surgical removal	MALT		Surgical removal	Clinical follow-up
19/50 years/Female	No	Chest pain for 1 year	RUL	6.9 × 6.3 cm	Transbronchial biopsy	MALT		Chemotherapy	Significantly decreased lesion size on chest CT images obtained after four cycles of chemotherapy

(continued)

Table 1. Continued.

No./Age/Sex	Smoking history	Symptoms	Characteristics and distribution of lesions	Tumor size	Source of specimen	Pathological diagnosis	PET-SUV SUVmax	Treatment	Prognosis
20/60/Male	10 cigarettes/day for 35 years	Intermittent fatigue for 6 years with occasional cough with a little white sputum	Consolidation in the RML, RLL, and LUL	8.0 × 4.9 cm	CT-guided needle biopsy	MALT	3.1–3.8	Treatment after discharge	Telephone follow-up
21/54/Female	No	Shortness of breath for several weeks	Patchy opacities in BL	7.7 × 5.5 cm	CT-guided needle biopsy	MALT		Treatment after discharge	Telephone follow-up
22/53/Female	No	Detected incidentally Previous lupus nephritis, diabetes, and rheumatoid arthritis	Masses in the LUL	5.2 3.4 cm	CT-guided needle biopsy	MALT	3.0	Surgical removal	Telephone follow-up

CT, computed tomography; PET, positron emission tomography; RUL, right upper lobe; RML, right middle lobe; RLL, right lower lobe; LUL, left upper lobe; LLL, left lower lobe; BL, both lungs; SUVmax, maximum standardized uptake value; CIK, cytokine-induced killer; MALT, mucosa-associated lymphoid tissue; DLBCL, diffuse large B-cell lymphoma; PR, partial remission; CMR, complete metabolic remission; DS, Deauville Scale

pathologically diagnosed with PPL after CT-guided needle biopsy (14 patients), surgical removal (6 patients), or transbronchial biopsy (2 patients).

The chest CT scans of the 22 patients (Table 2) demonstrated a single lesion in the lungs in 11 patients (3 in the left upper lobe, 3 in the left lower lobe, 4 in the right upper lobe, and 1 in the right lower lobe) (Figure 1) and multiple lesions in 11 patients (1 in the right upper lobe, 2 in the left upper lobe + both lower lobes, 2 in both upper lobes + both lower lobes, 2 in the right upper lobe + right middle lobe + right lower lobe, 1 in both upper lobes + the right lower lobe, 1 in the right upper lobe + left upper lobe, 1 in the right upper lobe + both lower lobes, and 1 in the left upper lobe + right middle lobe) (Figure 2). The right upper lobe was involved in 11 patients. Eleven patients showed pulmonary nodules and masses, and intralesional air bronchograms were identified in 4 of them; 10 patients showed ill-defined patches of exudative lesions and consolidation along the bronchovascular bundle, and intralesional air bronchograms were identified in 6 of them. One patient showed multiple nodules, masses, and patches in the lungs, with air bronchograms in part of the lesions. Twelve patients showed ill-defined areas of ground-glass, brush-like changes (Figure 3-1 and 3-2). Thirteen patients showed lobulation and a speculation sign around the lesion, 12 showed a bronchial inflation sign, 2 showed bronchiectasis, 4 showed bronchiectomy, 1 showed necrosis, 5 showed a vascular floating sign, and 1 showed pleural effusion after enhanced scanning. The possibility of lymphoma was considered based on the chest CT findings of only five patients; other diagnoses included inflammatory and infectious lesions (13 patients), lung cancer (3 patients), and a tumorous lesion for which needle biopsy was recommended (1 patient). Eleven patients underwent an ^{18}F-FDG PET/CT

scan, and lesions with an SUVmax of >10 were detected in four patients. The SUVmax ranged from 2.25 to 9.54 in the remaining seven patients.

Of the 22 patients, 14 underwent CT-guided needle biopsy, 6 underwent surgical removal, and 2 underwent transbronchial biopsies. All cases of PPL were pathologically classified as NHL; 16 were MALT, 3 were diffuse large B-cell lymphoma, and 3 were NK/T-cell lymphoma. Of the six patients who underwent surgical removal, five reported no sign of relapse in telephone follow-ups. However, one with multiple lung lesions showed multiple areas of consolidation in the lungs with irregular concentration of radioactivity (indicating possible residual malignancy) in PET/CT scanning performed after three cycles of R-CHOP chemotherapy and four cycles of autologous cytokine-induced killer cell-based immunotherapy following right upper lobectomy. Eleven patients received three to four cycles of chemotherapy, and the follow-up PET/CT revealed smaller lesions and diminishment of the metabolic rate to various degrees in eight patients. One patient showed significantly smaller bilateral parenchymal lung and pleural lesions and a diminished metabolic rate; however, a CT scan performed at a local hospital 2 years later showed enlarged masses, and the possibility of relapse could not be excluded. Another patient died following an exacerbation after 1 week of COP+L chemotherapy. Two representative cases are described below.

In Case 1, the patient presented with a cold with cough and fever. Chest CT revealed ill-defined irregular masses and areas of consolidation in the posterior segment of the right upper lobe and the dorsal and posterior basal segments of the right lower lobe. Air bronchograms were present in the lesion in the right upper lobe, the distal bronchi were obstructed, and the proximal bronchi were mildly dilated and

Table 2. CT features of primary pulmonary lymphoma in 22 patients

No.	Distribution of lesions and characteristics	Halo sign	Burrs and leaves	Air bronchial sign	Bronchiectasia	Calcification	Necrosis and cavity	Bronchiectomy	Vascular floating sign	Pleural effusion	CT diagnosis
1	RUL, RML, RLL, LLL/nodular mass	Yes	No	Yes	No	No	No	No	/	No	Inflammatory lesions
2	RUL, RML, RLL/patchy mass	Yes	Yes	Yes	No	No	No	No	Yes	No	Diffuse lung cancer
3	BL/patchy, ground-glass opacity	Yes	No	Yes	No	No	No	No	/	Yes	Infectious lesions
4	LLL/honeycomb consolidation	No	Yes	Yes	Yes	No	Yes	Yes	/	No	Chronic inflammation
5	RUL, LUL/patchy	Yes	Yes	Yes	No	No	No	No	/	No	Inflammatory lesions
6	RUL, RLL, LLL/nodule ground-glass opacity	Yes	Yes	No	No	No	No	No	/	No	Inflammatory granuloma
7	RUL/nodule	Yes	Yes	No	No	No	No	No	No	No	Inflammatory lesions
8	LLL/nodule	Yes	Yes	Yes	No	No	No	Yes	/	No	Lymphoma
9	LUL/mass	No	Yes	No	No	No	No	No	No	No	Central lung cancer
10	BL/patchy and nodule	Yes	Yes	Yes	Yes	No	No	No	/	No	Infectious lesions
11	LUL, RLL, LLL/ nodule and mass	Yes	No	No	No	No	No	No	Yes	No	Lymphoma
12	RUL, RML/mass	No	No	No	No	No	No	Yes	/	No	Lymphoma
13	LUL/nodule	Yes	Yes	No	No	No	No	No	Yes	No	Lung cancer
14	RUL/nodule	No	No	No	No	No	No	No	/	No	Lymphoma
15	RLL, LUL, LLL/ nodule, mass	No	No	No	No	No	No	No	No	No	Lymphoma
16	RLL/mass	Yes	Yes	Yes	No	No	No	No	Yes	No	Inflammation
17	RUL/patchy	No	No	No	No	No	No	No	/	No	Inflammation
18	LLL/mass	No	Yes	Yes	No	No	No	No	Yes	No	Infectious lesions
19	RUL/consolidation	No	No	Yes	No	No	No	No	/	No	Pneumonia
20	RML, RLL, LUL/ consolidation	Yes	Yes	Yes	No	No	No	No	/	No	Infectious lesions
21	BL/patchy	No	No	No	No	No	No	Yes	/	No	Infectious lesions
22	LUL/mass	Yes	Yes	Yes	No	No	No	No	/	No	Tumorous lesions

CT, computed tomography; RUL, right upper lobe; RML, right middle lobe; RLL, right lower lobe; LUL, left upper lobe; LLL, left lower lobe; BL, bilateral lung; /, no enhancement check was performed
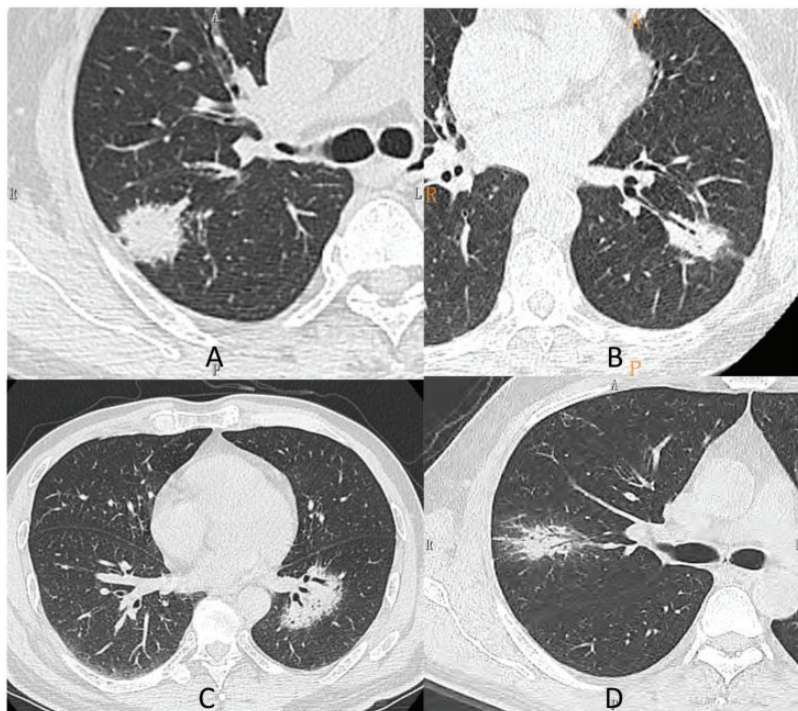
Figure 1. (a–d) Single nodule and mass in the lungs of four patients

distorted (Figure 4-1 and 4-2). The patient was diagnosed with multiple inflammatory lesions in the right lung. PET/CT then revealed a large area of hypermetabolic consolidation in the posterior segment of the right upper lobe and areas of soft tissue density with variable metabolic activity in the dorsal and posterior basal segments of the right lower lobe. Thus, the possibility of malignancy (MALT) could not be excluded. A transbronchial biopsy was performed 20 days later, and the pathologic examination revealed infiltration of uniformly sized lymphocytes into the respiratory epithelium and lamina propria as well as lymphoepithelial lesions, which were probably MALT based on correlation with the immunohistochemistry results. A PET/CT scan performed after the patient had received three cycles of R-COP chemotherapy demonstrated metabolic activity in

the original lesions. The patient then developed a pulmonary infection after three cycles of R-F chemotherapy and was given anti-infection treatment. A chest CT scan performed after the treatment demonstrated a reduced degree of consolidation and patent bronchi.

In Case 13, a left lung nodule was found during a physical examination at a local hospital. The patient then developed productive phlegm, hemoptysis, and chest pain of unknown cause after taking Chinese medicine for 3 months. A follow-up CT scan performed 6 months later revealed enlargement of the left lung nodule. Plain and contrast-enhanced chest CT scans showed a nodule of about 20×34 mm with a CT value of about 50 HU in the left upper lobe. The nodule exhibited mild heterogeneous enhancement in the contrast-enhanced scan, with a CT value of about 63
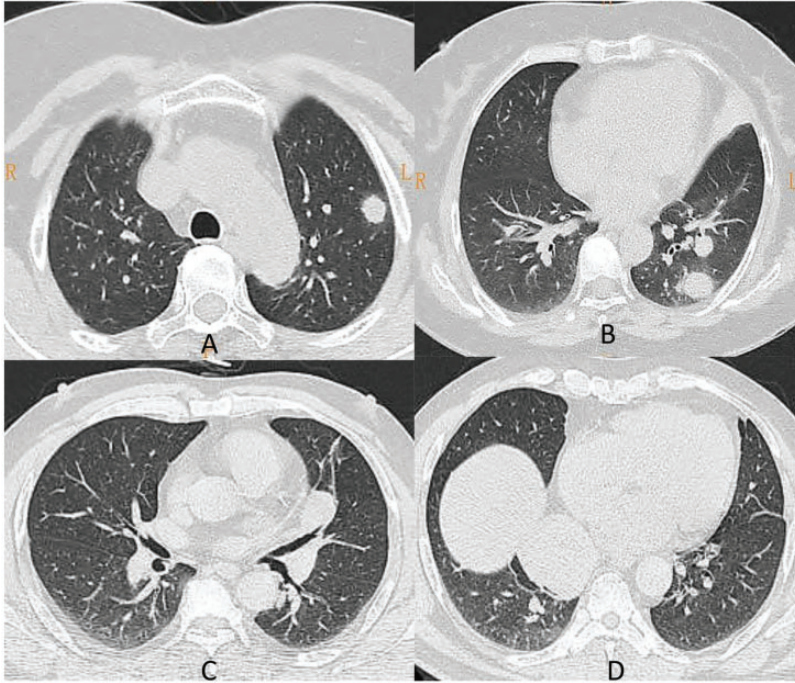
Figure 2. (a–d) Multiple nodules and masses in the lungs. (a, b) and (c, d) are the images of different layers of two patients, respectively

HU and lobulation and convergence of blood vessels; these findings were suggestive of lung cancer (Figure 5). Video-assisted thoracoscopic left upper lobectomy and lymphadenectomy were subsequently performed. The pathology report revealed B-cell NHL of $3.5 \times 2.5 \times 2.5$ cm in the left upper lobe, possibly germinal center-derived diffuse large B-cell lymphoma, invading the visceral pleura. No tumor was detected in the bronchial stump. No lymph node involvement was found in the submitted specimen.

Discussion

The most common form of PPL is MALT lymphoma, a subtype of NHL, which represents 70% to 80% of all PPLs.[8] Brienenstock et al.[9] first described MALT in 1973. Most researchers hold that MALT does not arise in pulmonary tissues and may develop secondary to chronic inflammation, smoking, autoimmune diseases, and other risk factors.[10] Additionally, lymphoproliferative diseases (including NHL and other lymphomas) can reportedly be detected during the treatment of rheumatoid arthritis with methotrexate. In 48 patients undergoing treatment with methotrexate for rheumatoid arthritis, the rheumatoid arthritis progressed to lymphoproliferative diseases, 4 of which were primary.[11] This finding suggests that methotrexate-induced hypoimmunity may contribute to the development and expansion of a malignant lymphocyte clone.[11]

The radiological manifestations and underlying pathology of PPL can be divided into five categories.[12] (1) The first is the mass and nodular type. When the peribronchovascular lymphoma cells infiltrate and spread
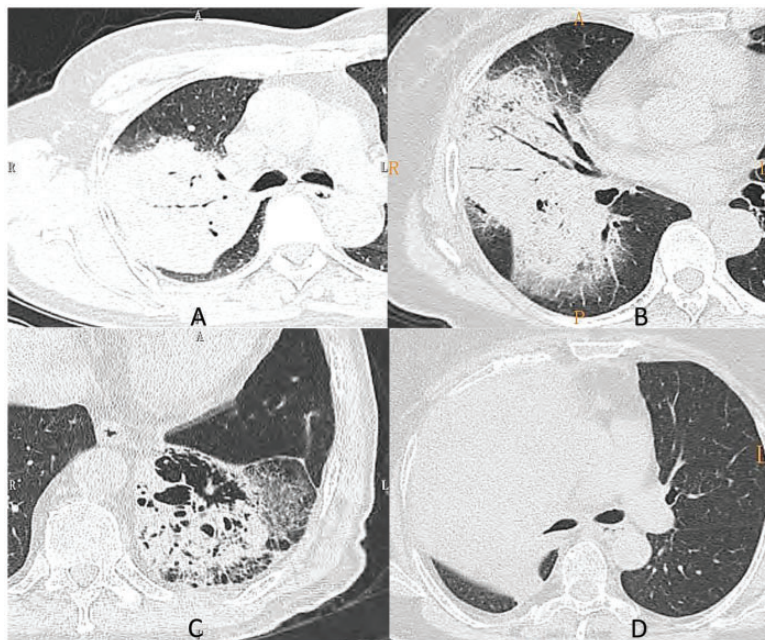
Figure 3-1. (a–d) Patches and consolidation in the lungs

along the peribronchovascular lymph sinus, the peribronchovascular tissues thicken, forming nodules or masses. These manifest as single or multiple well- or ill-defined quasi-circular nodules and masses in the pulmonary interstitium near the bronchus or subpleural areas, with air bronchograms in lesions of >1 cm. (2) In the pneumonic-alveolar type, bronchial submucosal lymphoma cells damage the bronchial basement membrane and epithelium, forming a nodular bump in the lumen. This leads to deformation, stenosis, and even occlusion of the lumen; pulmonary consolidation or atelectasis; and obstructive pneumonia-like changes. The condition manifests as ill-defined patchy exudative lesions and/or consolidated masses. (3) In the bronchovascular-lymphangitic type, lymphoma cells infiltrate the peribronchial interstitium. The resultant lesions present as diffuse fine or coarse reticulate or small reticulonodular structures extending outward from the hilum or as ground-glass changes with thickening and distortion of the bronchovascular bundle. (4) The miliary type presents as multiple small (<3-mm) miliary nodules in a linear diffuse distribution along the bronchus. The nodules have rough boundaries and no air bronchograms. (5) Finally, the mixed type is a combination of two or more of the above four types. Consolidation-type PPL reportedly represents about 17% of all PPLs.[13] In the present study, however, nearly 50% of patients showed nodules and masses or peribronchial consolidation, and 11 of the 16 patients with MALT showed nodules and masses or consolidation, which is a characteristic finding. In our series, intralesional air bronchograms were observed in 14 patients, and ground-glass brush-like changes were observed in 12 patients.[6] PPL arises in the lymphatic tissues in the submucosa of bronchi or around the bronchial arteries and veins, infiltrates and spreads along the lymphatic network, and invades the pulmonary interstitium outside
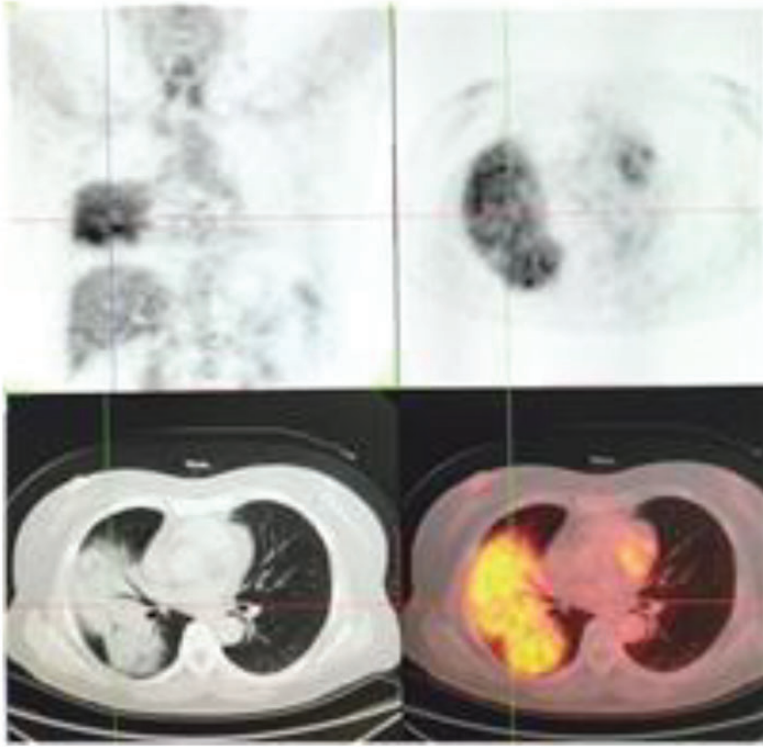
Figure 3-2. Positron emission tomography/computed tomography image of pneumonic pulmonary lymphoma (corresponding to Figure 3-1(b))
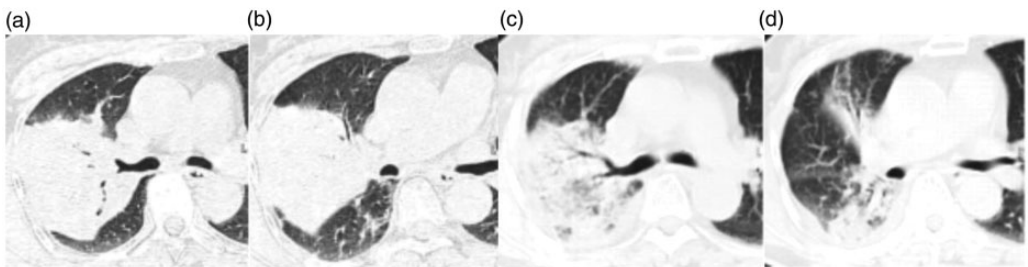

Figure 4-1. (a, b) Main level of the first chest computed tomography image of the patient on 20 November 2010. (c, d) Chest computed tomography image of the patient who developed pulmonary infection after three courses of R-COP3 and R-F chemotherapy on 28 June 2013

the bronchial wall. Therefore, the lesion usually shows dilation and distortion of the bronchus only; it rarely shows bronchial cut-off and obstruction caused by tumor infiltration-induced alveolar collapse and damage to the peribronchial parenchyma.[10] Interstitial changes are often present around the lesion.

PET/CT can detect most forms of lymphomas, especially the high-malignancy
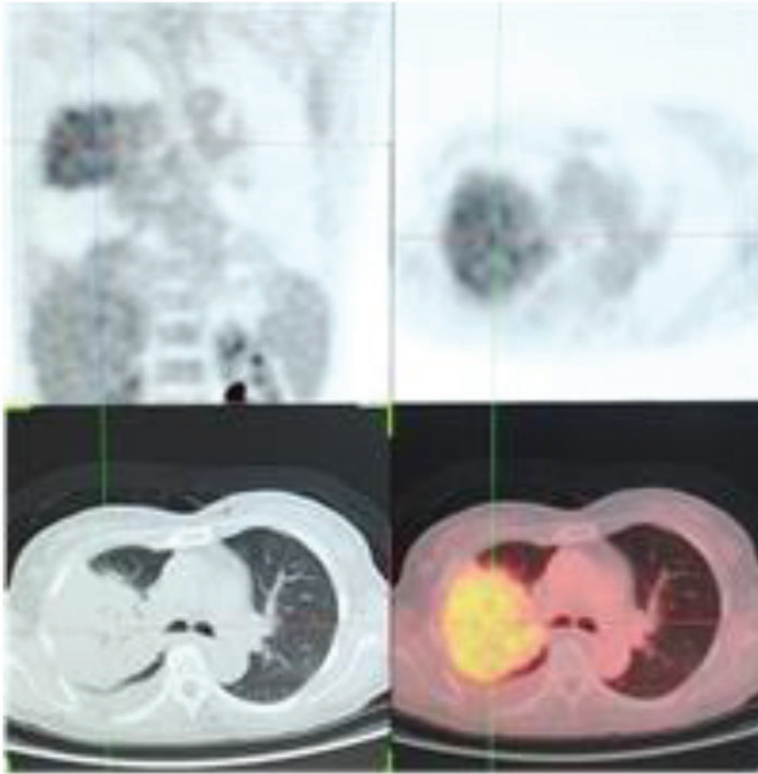
Figure 4-2. Review of positron emission tomography/computed tomography after three courses of R-COP regimen chemotherapy
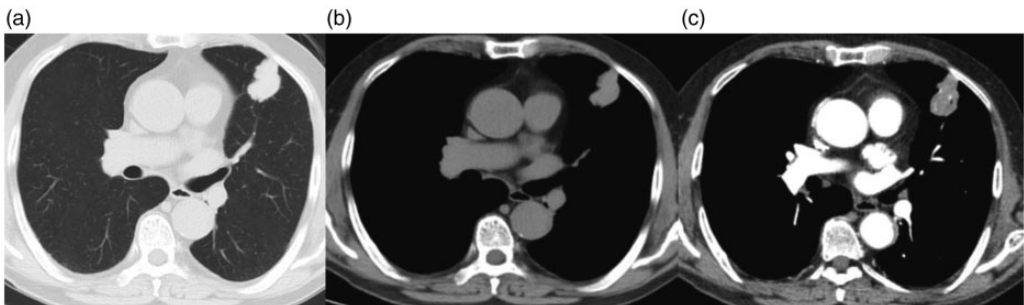
Figure 5. Chest computed tomography plain scan image (lung window and mediastinal window) and enhanced arterial-phase image of the patient on 1 February 2017

pathological types; however, its usefulness in detecting MALT lymphoma remains controversial.[14–18] Of the 11 patients who underwent PET/CT in the present study, 4 patients (2 with diffuse large B-cell lymphoma and 2 with NK/T cell lymphoma) were diagnosed with a pathological type with an SUVmax of >10; this was significantly

higher than the SUVmax of MALT lymphoma (range of 2.23–7.70). To some extent, this finding indicates that pathological types of higher malignancy have a higher concentration of tracer in the lesion. Additionally, because the lung tissue is rich in gas-containing organs, the background radioactivity level is low, and there is no interference of physiological uptake. Even if the radioactivity uptake of the lesion is low, it can produce enough contrast. Therefore, despite the low degree of malignancy of pulmonary MALT lymphoma, if the course of the disease is long enough to develop into a larger lesion (enough to ingest more imaging agents), an adequate concentration of radioactivity will be produced. ^{18}F-FDG PET/CT can cover the whole body and sensitively show the presence or absence of lesions in other parts of the body. Therefore, it has certain advantages in differentiating PPL from secondary pulmonary lymphoma. Notably, however, ^{18}F-FDG PET imaging is nonspecific, and other lung lesions (such as lung cancer, inflammation, tuberculosis, and others) can also produce radioactivity concentration. It is often impossible to accurately identify these lesions using only PET/CT images. The combination of clinical data and CT imaging features is needed to reduce the misdiagnosis rate.

The prognosis of PPL depends mainly on the type of leading lymphocytes and the stage of the disease. Most PPLs are of low malignancy and progress slowly. The therapeutic methods include surgical removal, radiotherapy, and chemotherapy. Surgical removal is mostly adopted for patients with focal lesions. Kawashina et al.[19] indicated that surgical removal should be chosen whenever possible for patients who can tolerate surgical procedures because it allows removal of the lesion and acquisition of definitive pathological findings, providing the basis for further treatment with radiotherapy. Chemotherapy is mostly chosen for patients with multiple lesions and involvement of both lungs; CHOP chemotherapy (cyclophosphamide, doxorubicin, vincristine, and prednisolone) is most commonly used. In the present series, 10 patients underwent chemotherapy and follow-up examinations, and a 75-year-old woman died because her condition worsened after chemotherapy. The other patients showed improvement of their clinical symptoms, CT suggested changes in uptake, and PET/CT demonstrated diminished metabolic activity.

PPL is rare and lacks characteristic clinical and radiologic manifestations, although adequate radiologic data will provide diagnostic clues that lead the clinician to a diagnosis. The possibility of PPL should be considered in middle-aged and advanced-age patients with all of the following: (1) risk factors such as chronic inflammation, smoking, or autoimmune diseases; (2) mild clinical symptoms; (3) single or multiple ill-defined lesions (nodules and masses or patchy opacities) with intralesional air bronchograms, mild to moderate enhancement after the administration of contrast agents, and normal coursing of vessels in the pulmonary interstitium around the bronchus, in the subpleural areas, or involving the right upper lobe; (4) variable manifestations (multiple lesions); (5) no significantly enlarged mediastinal lymph nodes; (6) exclusion of common diseases according to the clinical medical history and PET/CT findings; and (7) no significant change of the lung lesion after short-term anti-inflammatory treatment.

Abbreviations

PPL, primary pulmonary lymphoma; NHL, non-Hodgkin's lymphoma; MALT, mucosa-associated lymphoid tissue; CT, computed tomography; PET, positron emission tomography; FDG,

fluorodeoxyglucose; SUVmax, maximum standardized uptake value

Compliance with ethical standards

Because this was a retrospective study, the ethics committees of all three hospitals waived the requirement for informed consent. This study was conducted in compliance with the institutional policy regarding the protection of patients' confidential information and was approved by the Research Ethics Committee of Beijing Shijitan Hospital affiliated to Capital Medical University. All procedures were carried out in accordance with the approved guidelines of Beijing Shijitan Hospital affiliated with Capital Medical University.

ORCID iD

Jun Han   https://orcid.org/0000-0001-6393-7042

References

1. Miller DL and Allen MS. Rare pulmonary neoplasms. *Mayo Clin Proc* 1993; 68: 492–498.
2. Kocatürk Cİ, Seyhan EC ,Günlüoğlu MZ, et al. Primary pulmonary non-Hodgkin's lymphoma: ten cases with a review of the literature. *Tuberk Toraks* 2012; 60: 246–253.
3. Hansmann ML, Zwingers T and Lennert K. Primary lymphomas of the lung; morphological and clinical features. *Histopathology* 1990; 16: 519–531.
4. Freeman C, Berg JW and Curler SJ. Occurrence and prognosis of extra-nodal lymphomas. *Cancer* 1972; 29: 252–260.
5. Kligerman SJ, Franks TJ and Galvin JR. Primary extranodal lymphoma of the thorax. *Radiol Clin North Am* 2016; 54: 673–687.
6. Zhang WD, Guan YB, Li CX, et al. Pulmonary mucosa-associated lymphoid tissue lymphoma: computed tomography and 18F fluorodeoxyglucose-positron emission tomography/computed tomography imaging findings and follow-up. *J Comput Assist Tomogr* 2011; 35: 608–613.
7. Cordier JF, Chailleuz E, Lanque D, et al. Primary pulmonary lymphomas. A clinical study of 70 cases in nonimmunocompromised patients. *Chest* 1993; 103: 201–208.
8. Kurtin PJ, Myers JL, Adlakha H, et al. Pathologic and clinical features of primary pulmonary extranodal marginal zone B-cell lymphoma of MALT type. *Am J Surg Pathol* 2001; 25: 997–1008.
9. Brienenstock J, Johnston N, Perey D, et al. Bronchial lymphoid tissue. *Lab Lancet* 2013; 28: 686–689.
10. Wislez M, Cadranel J, Antoine M, et al. Lymphoma of pulmonary mucosa-associated lymphoid tissue: CT scan findings and pathological correlations. *Eur Respir J* 1999; 14: 423–429.
11. Hoshida Y, Xu JX, Fujita S, et al. Lymphoproliferative disorders in rheumatoid arthritis: clinicopathological analysis of 76 cases in relation to methotrexate medication. *J Rheumatol* 2007; 34: 322–331.
12. Bae YA, Lee KS, Han J, et al. Marginal zone B-cell lymphoma of bronchus-associated lymphoid tissue: imaging findings in 21 patients. *Chest* 2008; 133: 433–440.
13. Ferraro P, Trastek VF, Adlakha H, et al. Primary non-Hodgkin's lymphoma of the lung. *Ann Thorac Surg* 2000; 69: 993–997.
14. Beal KP, Yeung HW, Yahalom J, et al. FDG-PET scanning for detection and staging of extranodal marginal zone lymphomas of the MALT type: a report of 42 cases. *Ann Oncol* 2005; 16: 473–480.
15. Hoffmann M, Wöhrer S, Becherer A, et al. ^{18}F-Fluoro-deoxy-glucose positron emission tomography in mucosa-associated lymphoid

tissue: histology makes the difference. *Ann Oncol* 2006; 17: 1761–1765.

16. Perry C, Herishanu Y, Metzer U, et al. Diagnostic accuracy of PET/CT in patients with extranodal marginal zone MALT lymphoma. *Eur J Haematol* 2007; 79: 205–209.

17. Yoon RG, Kim MY, Song JW, et al. Primary endobronchial marginal zone B-cell lymphoma of bronchus-associated lymphoid tissue: CT findings in 7 patients. *Korean J Radiol* 2013; 14: 366–374.

18. Albano D, Borghesi A, Bosio G, et al. Pulmonary mucosa-associated lymphoid tissue lymphoma: 18F-FDG PET/CT and CT findings in 28 patients. *Br J Radiol* 2017; 90: 20170311.

19. Kawashina O, Hirai T and Kamiyoshihara M. Early primary pulmonary lymphoma. *Oncol Rep* 1998; 5: 135–138.